Eur. Phys. J. C (2017) 77:548
DOI 10.1140/epjc/s10052-017-5119-8

THE EUROPEAN PHYSICAL JOURNAL C

CrossMark

Regular Article - Theoretical Physics

High-p_T dilepton tails and flavor physics

Admir Greljo[1,2], **David Marzocca**[1,a]

[1] Physik-Institut, Universität Zürich, Zürich 8057, Switzerland
[2] Faculty of Science, University of Sarajevo, Zmaja od Bosne 33-35, 71000 Sarajevo, Bosnia and Herzegovina

Received: 24 June 2017 / Accepted: 14 July 2017 / Published online: 16 August 2017
© The Author(s) 2017. This article is an open access publication

Abstract We investigate the impact of flavor-conserving, non-universal quark-lepton contact interactions on the dilepton invariant mass distribution in $p\,p \to \ell^+\ell^-$ processes at the LHC. After recasting the recent ATLAS search performed at 13 TeV with 36.1 fb^{-1} of data, we derive the best up-to-date limits on the full set of 36 chirality-conserving four-fermion operators contributing to the processes and estimate the sensitivity achievable at the HL-LHC. We discuss how these high-p_T measurements can provide complementary information to the low-p_T rare meson decays. In particular, we find that the recent hints on lepton-flavor universality violation in $b \to s\mu^+\mu^-$ transitions are already in mild tension with the dimuon spectrum at high-p_T if the flavor structure follows minimal flavor violation. Even if the mass scale of new physics is well beyond the kinematical reach for on-shell production, the signal in the high-p_T dilepton tail might still be observed, a fact that has been often overlooked in the present literature. In scenarios where new physics couples predominantly to third generation quarks, instead, the HL-LHC phase is necessary in order to provide valuable information.

1 Introduction

Searches for new physics in flavor-changing neutral currents (FCNC) at low energies set strong limits on flavor-violating semileptonic four-fermion operators $(qq'\ell\ell)$, often pushing the new physics mass scale Λ beyond the kinematical reach of the LHC [1]. For example, if the recent hints for lepton-flavor non-universality in $b \to s\ell^+\ell^-$ transitions [2–5] are confirmed, the relevant dynamics might easily be outside the LHC range for on-shell production.

In this situation, an effective field theory (EFT) approach is applicable in the entire spectrum of momentum transfers in proton collisions at the LHC, including the most energetic processes. Since the leading deviations from the SM scale like $\mathcal{O}(p^2/\Lambda^2)$, where p^2 is a typical momentum exchange, less precise measurements at high-p_T could offer similar (or even better) sensitivity to new physics with respect to high-precision measurements at low energies. Indeed, opposite-sign same-flavor charged lepton production, $p\,p \to \ell^+\ell^-$ $(\ell = e, \mu)$, sets competitive constraints on new physics when compared to some low-energy measurements [6–8] or electroweak precision tests performed at LEP [9].

At the same time, motivated new physics flavor structures can allow for large flavor-conserving but flavor non-universal interactions. In this work we study the impact of such contact interactions on the tails of dilepton invariant mass distribution in $p\,p \to \ell^+\ell^-$ and use the limits obtained in this way to derive bounds on class of models which aim to solve the recent $b \to s\ell\ell$ anomalies. With a similar spirit, in Ref. [10] it was shown that the LHC measurements of $pp \to \tau^+\tau^-$ already set stringent constraints on models aimed at solving the charged-current $b \to c\tau\bar{\nu}_\tau$ anomalies. The paper is organized as follows. In Sect. 2 we present a general parameterization of new physics effects in $p\,p \to \ell^+\ell^-$ and perform a recast of the recent ATLAS search at 13 TeV with 36.1 fb^{-1} of data [11] to derive present and future-projected limits on flavor non-universal contact interactions for all quark flavors accessible in the initial protons. In Sect. 3 we discuss the implications of these results on the rare FCNC B meson decay anomalies. The conclusions are found in Sect. 4.

2 New physics in the dilepton tails

2.1 General considerations

We start the discussion on new physics contributions to dilepton production via Drell–Yan by listing the gauge-invariant dimension-six operators which can contribute at tree-level to the process. We opt to work in the Warsaw basis [12]. Neglecting chirality-flipping interactions (e.g. scalar or ten-

[a] e-mail: marzocca@physik.uzh.ch

sor currents, expected to be suppressed by the light fermion Yukawa couplings), dimension-six operators can contribute to $q\,\bar{q} \to \ell^+\ell^-$ either by modifying the SM contributions due to the Z exchange or via local four-fermion interactions. The former class of deviations can be probed with high precision by on-shell Z production and decays at both LEP-1 and LHC (see e.g. Ref. [13]). Also, such effects are not enhanced at high energies, scaling like $\sim v^2/\Lambda^2$, where $v \simeq 246$ GeV.

For these reasons we neglect them and focus on the four-fermion interactions which comprise four classes depending on the chirality: $(\bar{L}L)(\bar{L}L)$, $(\bar{R}R)(\bar{R}R)$, $(\bar{R}R)(\bar{L}L)$ and $(\bar{L}L)(\bar{R}R)$. In particular, the relevant set of operators is

$$\begin{aligned}\mathcal{L}^{\rm SMEFT} \supset\ & \frac{c^{(3)}_{Q_{ij}L_{kl}}}{\Lambda^2}(\bar{Q}_i\gamma_\mu\sigma^a Q_j)(\bar{L}_k\gamma^\mu\sigma_a L_l)\\ &+\frac{c^{(1)}_{Q_{ij}L_{kl}}}{\Lambda^2}(\bar{Q}_i\gamma_\mu Q_j)(\bar{L}_k\gamma^\mu L_l)\\ &+\frac{c_{u_{ij}e_{kl}}}{\Lambda^2}(\bar{u}_i\gamma_\mu u_j)(\bar{e}_k\gamma^\mu e_l)+\frac{c_{d_{ij}L_{kl}}}{\Lambda^2}(\bar{d}_i\gamma_\mu d_j)(\bar{e}_k\gamma^\mu e_l)\\ &+\frac{c_{u_{ij}L_{kl}}}{\Lambda^2}(\bar{u}_i\gamma_\mu u_j)(\bar{L}_k\gamma^\mu L_l)+\frac{c_{d_{ij}L_{kl}}}{\Lambda^2}(\bar{d}_i\gamma_\mu d_j)(\bar{L}_k\gamma^\mu L_l)\\ &+\frac{c_{Q_{ij}e_{kl}}}{\Lambda^2}(\bar{Q}_i\gamma_\mu Q_j)(\bar{e}_k\gamma^\mu e_l) \qquad (1)\end{aligned}$$

where i, j, k, l are flavor indices, $Q_i = (V^*_{ji}u^j_L, d^i_L)^T$ and $L_i = (\nu^i_L, \ell^i_L)^T$ are the SM left-handed quark and lepton weak doublets and d_i, u_i, e_i are the right-handed singlets. V is the CKM flavor mixing matrix and σ^a are the Pauli matrices acting on $SU(2)_L$ space.

An equivalent classification of the possible contact interactions can be obtained by studying directly the $q\,\bar{q} \to \ell^-\ell^+$ scattering amplitude:

$$\begin{aligned}&\mathcal{A}(q^i_{p_1}\bar{q}^j_{p_2}\to\ell^-_{p'_1}\ell^+_{p'_2})\\ &= i\sum_{q_L,q_R}\sum_{\ell_L,\ell_R}(\bar{q}^i\gamma^\mu q^j)\,(\bar{\ell}\gamma_\mu\ell)\,F_{q\ell}(p^2), \qquad (2)\end{aligned}$$

where $p \equiv p_1 + p_2 = p'_1 + p'_2$, and the form factor $F_{q\ell}(p^2)$ can be expanded around the physical poles present in the SM (photon and Z boson propagators), leading to

$$F_{q\ell}(p^2) = \delta^{ij}\frac{e^2 Q_q Q_\ell}{p^2} + \delta^{ij}\frac{g^q_Z g^\ell_Z}{p^2 - m^2_Z + i m_Z\Gamma_Z} + \frac{\epsilon^{q\ell}_{ij}}{v^2}. \qquad (3)$$

Here, $Q_{q(\ell)}$ is the quark (lepton) electric charge and $g^{q(\ell)}_Z$ is the corresponding coupling to Z boson: in the SM $g^f_Z = \frac{2m_Z}{v}(T^3_f - Q_f\sin^2\theta_W)$. The contact terms $\epsilon^{q\ell}_{ij}$ are related to the EFT coefficients in Eq. (1) by simple relations $\epsilon_x = \frac{v^2}{\Lambda^2}c_x$. The only constraint on the contact terms imposed by $SU(2)_L$ invariance are $\epsilon^{d_L e^k_R}_{ij} = \epsilon^{u_L e^k_R}_{ij} = c_{Q_{ij}e_{kk}}v^2/\Lambda^2$.

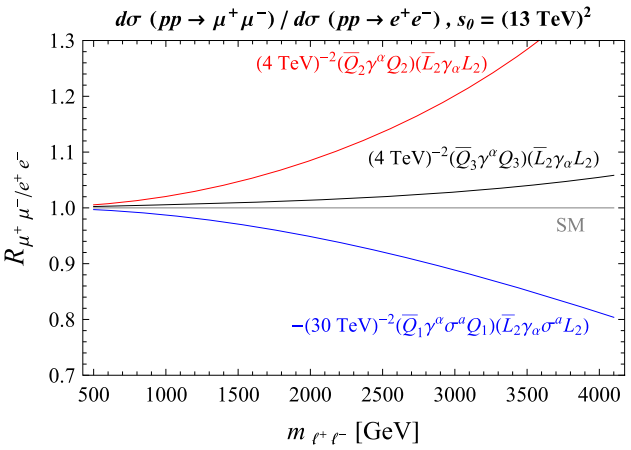

Fig. 1 $R_{\mu^+\mu^-/e^+e^-}$ as a function of the dilepton invariant mass $m_{\ell^+\ell^-}$ for three new physics benchmark points. See text for details

The dilepton invariant mass spectrum can be written (see Appendix A),

$$\frac{{\rm d}\sigma}{{\rm d}\tau} = \left(\frac{{\rm d}\sigma}{{\rm d}\tau}\right)_{\rm SM}\times\frac{\sum_{q,\ell}\mathcal{L}_{q\bar{q}}(\tau,\mu_F)|F_{q\ell}(\tau s_0)|^2}{\sum_{q,\ell}\mathcal{L}_{q\bar{q}}(\tau,\mu_F)|F^{\rm SM}_{q\ell}(\tau s_0)|^2}, \qquad (4)$$

where $\tau \equiv m^2_{\ell^+\ell^-}/s_0$ and $\sqrt{s_0}$ is the proton–proton center of mass energy. The sum is over the left- and right-handed quarks and leptons as well as the quark flavors accessible in the proton. Note that, since we are interested in the high-energy tails (away from the Z pole), the universal higher-order radiative QCD corrections factorize to a large extent. Therefore, consistently including those corrections in the SM prediction is enough to achieve good theoretical accuracy. It is still useful to define the differential LFU ratio,

$$\begin{aligned}R_{\mu^+\mu^-/e^+e^-}(m_{\ell\ell}) &\equiv \frac{{\rm d}\sigma_{\mu\mu}}{{\rm d}m_{\ell\ell}}\Big/\frac{{\rm d}\sigma_{ee}}{{\rm d}m_{\ell\ell}}\\ &= \frac{\sum_{q,\mu}\mathcal{L}_{q\bar{q}}(m^2_{\ell\ell}/s_0,\mu_F)|F_{q\mu}(m^2_{\ell\ell})|^2}{\sum_{q,e}\mathcal{L}_{q\bar{q}}(m^2_{\ell\ell}/s_0,\mu_F)|F_{qe}(m^2_{\ell\ell})|^2}, \qquad (5)\end{aligned}$$

which is a both theoretically and experimentally cleaner observable. In fact, in the SM both QCD and electroweak corrections are universal among muons and electrons, predicting $R^{\rm SM}_{\mu^+\mu^-/e^+e^-}(m_{\ell\ell}) \simeq 1$ with very high accuracy. As an illustration, in Fig. 1 we show the predictions for this observable at $\sqrt{s_0} = 13$ TeV, assuming new physics in three benchmark operators. The parton luminosities used to derive these predictions are discussed in the next chapter.

A goal of this work is to connect the high-p_T dilepton tails measurements with the recent experimental hints on lepton-flavor universality violation in rare semileptonic B meson decays. The pattern of observed deviations can be explained with a new physics contribution to a single four-fermion $bs\mu\mu$ contact interaction. As discussed in more detail in Sect. 3, a good fit of the flavor anomalies can be obtained with a left-handed chirality structure. For this reason, when

discussing the connection to flavor in Sect. 3, we limit our attention to the $(\bar{L}L)(\bar{L}L)$ operators with muons given in the first line of Eq. (1).[1] To this purpose it is useful to rearrange the terms relevant to $p\,p \to \mu^+\mu^-$ as[2]:

$$\mathcal{L}^{\rm eff} \supset \frac{\mathbf{C}^{U\mu}_{ij}}{v^2}(\bar{u}^i_L\gamma_\mu u^j_L)(\bar{\mu}_L\gamma^\mu\mu_L) + \frac{\mathbf{C}^{D\mu}_{ij}}{v^2}(\bar{d}^i_L\gamma_\mu d^j_L)(\bar{\mu}_L\gamma^\mu\mu_L). \tag{6}$$

The $\mathbf{C}^{U\mu}$ and $\mathbf{C}^{D\mu}$ matrices carry the flavor structure of the operators. Since the top quark does not appear in the process under study the corresponding terms can be neglected. Regarding the off-diagonal elements, we only keep the $b-s$ one, since it is where the flavor anomalies appear. We set the others to zero. In summary:

$$\mathbf{C}^{U\mu}_{ij} = \begin{pmatrix} C_{u\mu} & 0 & 0 \\ 0 & C_{c\mu} & 0 \\ 0 & 0 & C_{t\mu} \end{pmatrix}, \quad \mathbf{C}^{D\mu}_{ij} = \begin{pmatrix} C_{d\mu} & 0 & 0 \\ 0 & C_{s\mu} & C^*_{bs\mu} \\ 0 & C_{bs\mu} & C_{b\mu} \end{pmatrix}. \tag{7}$$

2.2 Present limits and HL-LHC projections

In this section we derive limits on the flavor non-universal quark-lepton contact interactions by looking in the tails of dilepton invariant mass distributions in $p\,p \to \ell^+\ell^-$ at the LHC. In our analysis we closely follow the recent ATLAS search [11] performed at 13 TeV with 36.1 fb^{-1} of data. We digitize Fig. 1 of Ref. [11], which shows the distribution of dielectron and dimuon reconstructed invariant masses after the final event selection. We perform a profile likelihood fit to a binned histogram distribution adopting the method from Ref. [14]. The number of signal events, as well as the expected signal events in the SM and background processes, are directly taken from Fig. 1 of Ref. [11]. The likelihood function (L) is constructed treating every bin as an independent Poisson variable, with the expected number of events,

$$\Delta N^{\rm bin} = \Delta N^{\rm bin}_{\rm SM} \times \frac{\sum_{q,\ell}\int_{\tau^{\rm bin}_{\rm min}}^{\tau^{\rm bin}_{\rm max}} {\rm d}\tau\ \tau\ \mathcal{L}_{q\bar{q}}(\tau,\mu_F)\ |F_{q\ell}(\tau s_0)|^2}{\sum_{q,\ell}\int_{\tau^{\rm bin}_{\rm min}}^{\tau^{\rm bin}_{\rm max}} {\rm d}\tau\ \tau\ \mathcal{L}_{q\bar{q}}(\tau,\mu_F)\ |F^{\rm SM}_{q\ell}(\tau s_0)|^2}, \tag{8}$$

which is a function of the contact interactions. The best fit point corresponds to the global minimum of $\chi^2 \equiv -2\log L$, while $n\sigma$ C.L. regions are given to be $\Delta\chi^2 \equiv \chi^2 - \chi^2_{\rm min} <$ $\Delta_{n\sigma}$, where $\Delta_{n\sigma}$ are defined with the appropriate cumulative distribution functions. In the numerical study we use the NNLO$_{118}$ MMHT2014 parton distribution functions set [15]. We checked that our results have a very small dependence on the factorization scale variation. At present, theoretical and systematic uncertainties on the expected number of events in the SM are negligible when compared to the statistical one in the high invariant mass region relevant for setting the limits on the contact interactions [9,11]. Nonetheless, their importance will increase at the high-luminosity phase. However, we still expect systematic uncertainties to be subleading or at most comparable to the statistical one. Therefore we do not include them in the projections.

Furthermore, we independently cross-check the results by implementing the subset of operators in Eqs. (6, 7) in a FeynRules [16] model, and generating $pp \to \mu^+\mu^-$ events at 13 TeV with the same acceptance cuts as in the ATLAS search [11] using MadGraph5_aMC@NLO [17]. We find good agreement between the fits performed in both ways.

In the SMEFT, neglecting flavor-violating interactions, are 18 independent four-fermion operators for muons and 18 for electrons relevant to $pp \to \ell^+\ell^-$ (see Eq. (1)). In Appendix B (Table 1) we provide present and projected 2σ limits on all these coefficients, using the recent ATLAS search [11]. While these limits are obtained in the scenario where only one operator is considered at a time, we checked that the 18×18 correlation matrix derived in the Gaussian approximation does not contain any large value (the only non-negligible correlations are among the triplet and singlet operators with the same-flavor content, which is discussed in more details below). The absence of flat directions can be understood by the fact that operators with fermions of different flavor or chirality do not interfere with each other.

Focusing only on the $(\bar{L}L)(\bar{L}L)$ operators (in the notation of Eq. (6)), the 2σ limits, both from the present ATLAS search (blue) and projected for 3000 fb^{-1} (red), are shown in Fig. 2. The solid lines show the 2σ bounds when operators are taken one at a time. The dashed ones show the limits when all the others are marginalized. The small difference between the two, especially with present accuracy, confirms what we commented above. Further constraints on the operators with $SU(2)_L$ triplet structure can be derived from the charged-current $pp \to \ell\nu$ processes [6,7,9].

3 Implications for $R(K)$ and $R(K^*)$

3.1 Effective field theory discussion

Recent measurements in rare semileptonic $b \to s$ transitions provide strong hints for a new physics contribution to $bs\mu\mu$ local interactions (see for example the recent analyses in Refs. [18–21]). In particular, a good fit of the anomaly in

[1] Note that similar conclusions apply also for solutions of the flavor anomalies involving operators with different chirality structure.

[2] The down and up couplings are given by two orthogonal combinations of the triplet and singlet operators in the first line of Eq. (1): $\mathbf{C}^{D(U)\mu}_{ij} = v^2/\Lambda^2(c^{(1)}_{Q_{ij}L_{22}} \pm c^{(3)}_{Q_{ij}L_{22}})$.

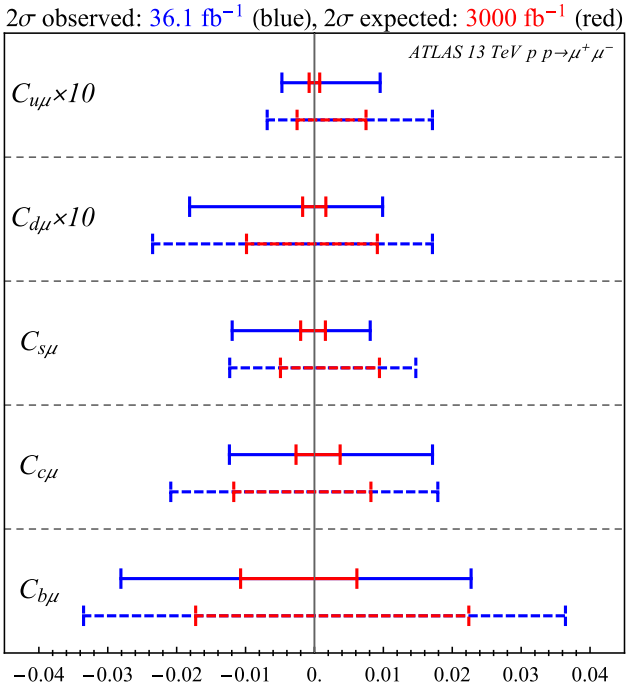

Fig. 2 In *blue* (*red*) we show the present (projected) 2σ limits on $C_{q\mu}$ (flavor conserving $(\bar{L}L)(\bar{L}L)$ operators) where $q = u, d, s, c$ and b, using 13 TeV ATLAS search in $pp \to \mu^+\mu^-$ channel [11]. *Dashed lines* show the limits when all other coefficients are marginalized, while the solid ones show the results of one-parameter fits

the differential observable P_5' [22], together with the hints on LFU violation in R_K and R_{K^*} [23–25], is obtained by considering a new physics contribution to the $C_{bs\mu}$ coefficient in Eqs. (6, 7). In terms of the SMEFT operators at the electroweak scale, this corresponds to a contribution to (at least) one of the two operators in the first row of Eq. (1) (see for example [26]). Moreover, the triplet operator could at the same time solve the anomalies in the charged-currrent $(R_{D^{(*)}})$, see e.g. Refs. [27–29].

Matching at the tree level this operator to the standard effective weak Hamiltonian describing $b \to s$ transitions, one finds

$$\Delta C_9^\mu = -\Delta C_{10}^\mu = \frac{\pi}{\alpha V_{tb} V_{ts}^*} C_{bs\mu}, \tag{9}$$

where α is the electromagnetic fine structure constant while $|V_{ts}| = (40.0 \pm 2.7) \times 10^{-3}$ and $|V_{tb}| = 1.009 \pm 0.031$ are CKM matrix elements [30].

The recent combined fit of Ref. [18] reported the best fit value and 1σ preferred range

$$\Delta C_9^\mu = -\Delta C_{10}^\mu = -0.61 \pm 0.12. \tag{10}$$

Using this result and Eq. (9) the scale of the relevant new physics can be estimated by defining $C_{bs\mu} = g_*^2 v^2/\Lambda^2$, obtaining $\Lambda/g_* \approx 32^{+4}_{-3}$ TeV. Depending on the value of g_*, i.e. from the particular UV origin of the operator, the scale of new physics Λ can be within or out of the reach of LHC direct searches. We show that, even in the latter case, under some assumptions it can be possible to observe an effect in the dimuon high-energy tail. When comparing low- and high-energy measurements, in principle the renormalization group effects should be taken into account. Since these effects in this case are small, we neglect them (see for example [26]).

We concentrate on UV models in which new particles are above the scale of threshold production at the LHC, such that the EFT approach is applicable in the most energetic dilepton events. We stress however, that even for models with light new physics these searches can be relevant.

We now focus on the flavor structure of the $\mathbf{C}_{ij}^{D(U)\mu}$ matrices in Eqs. (6, 7). New physics aligned only to the strange-bottom coupling $C_{bs\mu}$ will not be probed at the LHC, in fact the present (projected) 95% CL limits from the 13 TeV ATLAS $pp \to \mu^+\mu^-$ analysis with 36 fb^{-1} (3000 fb^{-1}) of luminosity are

$$\left| \frac{\pi}{\alpha V_{tb} V_{ts}^*} C_{bs\mu} \right| < 100\ (39), \tag{11}$$

which should be compared with the value extracted from the global flavor fits in Eq. (10). Such a peculiar flavor structure is possible but not very motivated from the model building point of view.

On the other hand, taking the $b \to s\mu^+\mu^-$ flavor anomalies at face value provides a measurement of the $C_{bs\mu}$ coefficient (via Eq. (9)). In most flavor models flavor-violating couplings are related (by symmetry or dynamics) to flavor-diagonal one(s). In this case the LHC upper limit on $|C_{q\mu}|$ from the dimuon high-p_T tail can be used in order to set a lower bound on $|\lambda_{bs}^q|$, defined as the ratio

$$\lambda_{bs}^q \equiv C_{bs\mu}/C_{q\mu}. \tag{12}$$

In the following we study such limits for several particularly interesting scenarios.

1. Minimal flavor violation

Under this assumption [31] the only source of flavor violation are the SM Yukawa matrices $Y_u \equiv V^\dagger \mathrm{diag}(y_u, y_c, y_t)$ and $Y_d \equiv \mathrm{diag}(y_d, y_s, y_b)$. Using a spurion analysis the following can be estimated

$$c_{Q_{ij}L_{22}}^{(3,1)} \sim \left(\mathbf{1} + \alpha Y_u Y_u^\dagger + \beta Y_d Y_d^\dagger \right)_{ij}, \tag{13}$$

where $\alpha, \beta \sim \mathcal{O}(1)$, which implies the following structure:

$$\begin{aligned} C_{u\mu} &= C_{c\mu} = C_{t\mu} \equiv C_{U\mu}, \\ C_{d\mu} &= C_{s\mu} = C_{b\mu} \equiv C_{D\mu}, \end{aligned} \tag{14}$$

while flavor-violating terms are expected to be CKM suppressed, for example $|C_{bs\mu}| \sim |V_{tb} V_{ts}^* y_t^2 C_{D\mu}|$. In this case the contribution to rare B meson decays has a V_{ts} suppression, while the dilepton signal at high-p_T receives an uni-

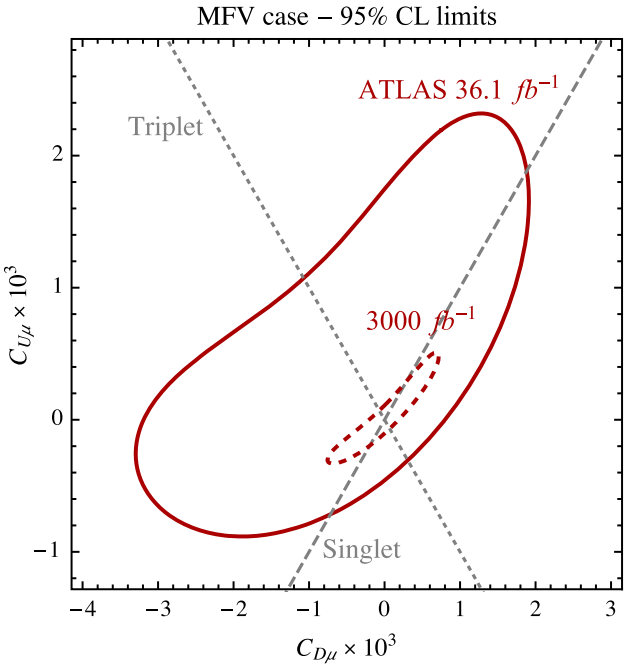

Fig. 3 Present and projected 95% CL limits from $pp \to \mu^+\mu^-$ in the MFV case defined by Eq. (14)

versal contribution dominated by the valence quarks in the proton. The flavor fit in Eq. (10) combined with this flavor structure would imply a value of $|C_{D\mu}| \sim 1.4 \times 10^{-3}$ which, as can be seen from the limits in Fig. 3, is already probed by the ATLAS dimuon search [11] depending on the origin of the operator (i.e. from the SU(2) singlet or triplet structure) and will definitely be investigated at high luminosity.[3] Allowing for more freedom and setting $C_{bs\mu} \equiv \lambda_{bs} C_{D\mu}$, we show in the top (central) panel of Fig. 4 the 95% CL limit in the $C_{D\mu}$–$|\lambda_{bs}|$ plane, where $C_{U\mu}$ is related to $C_{D\mu}$ by assuming the triplet (singlet) structure. As discussed before, a direct upper limit on λ_{bs} via $b - s$ fusion can be derived only for very large values. On the other hand, requiring $C_{bs\mu}$ to fit the B decay anomalies already probes interesting regions in parameter space, excluding the MFV scenario ($\lambda_{bs} = V_{ts}$) for both singlet and triplet cases.

2. $U(2)_Q$ **flavor symmetry**

This symmetry distinguishes light left-handed quarks (doublets) from third generation left-handed quarks (singlets). The leading symmetry-breaking spurion is a doublet whose flavor structure is unambiguously related to the CKM matrix [32]. In this case, in general the leading terms would involve the third generation quarks, as well as diagonal couplings in the first two generations. The relevant parameters

[3] It should also be noted that the triplet combination is bounded from the semileptonic hadron decays (CKM unitarity test) $C_{U\mu} - C_{D\mu} = (0.46 \pm 0.52) \times 10^{-3}$ [7], in the absence of other competing contributions.

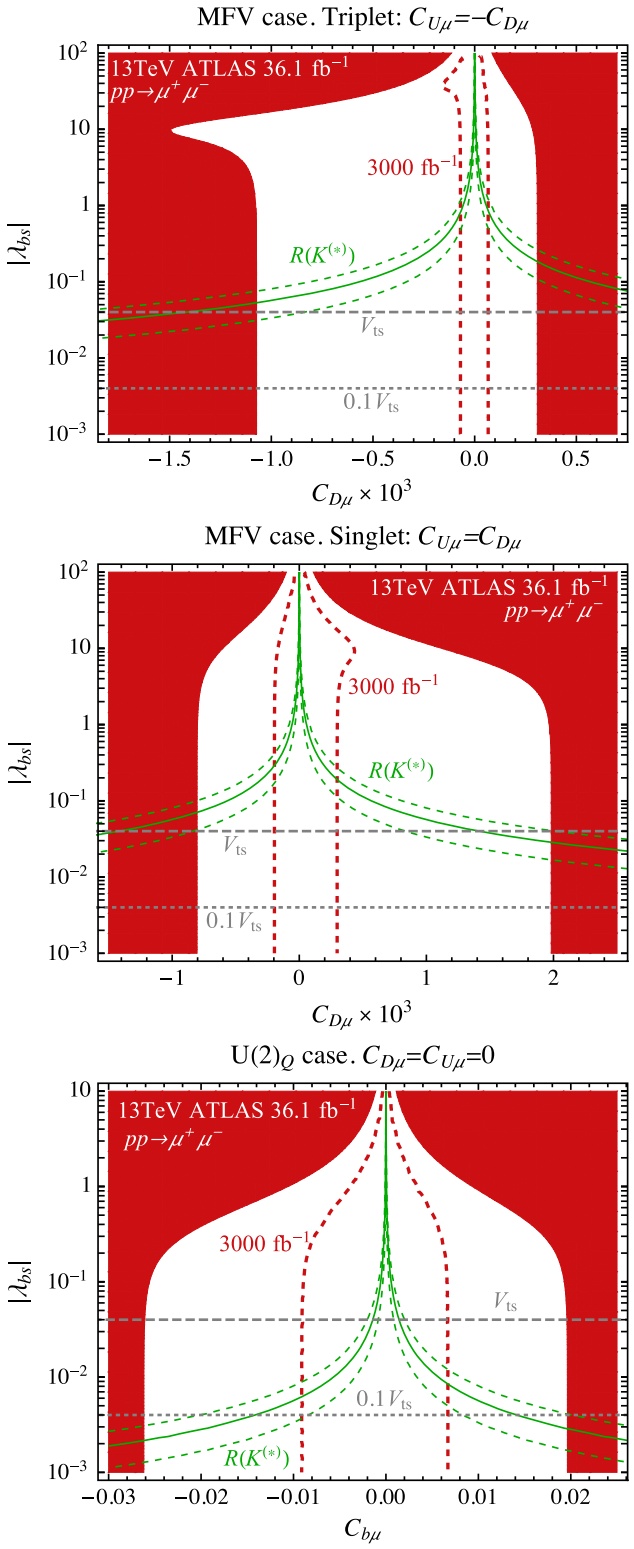

Fig. 4 We show the present (*solid red*) and projected (*dashed red*) 95% CL limit from $pp \to \mu^+\mu^-$ in the $C_{q\mu}$–$|\lambda_{bs}|$ plane. The *solid* (*dashed*) *green line* corresponds to the best fit (2σ interval) from the fit of the flavor anomalies in Eq. (10)

for the dimuon production would then be

$$C_{u\mu} = C_{c\mu} \equiv C_{U\mu}, \quad C_{d\mu} = C_{s\mu} \equiv C_{D\mu}, \quad C_{b\mu}, \quad C_{bs\mu} \equiv \lambda_{bs} C_{b\mu}, \tag{15}$$

where the flavor-violating coupling is expected to be $|\lambda_{bs}| \sim |V_{ts}|$. As already done in the MFV case, in the following we leave λ_{bs} free to vary and perform a four-parameter fit to the dimuon spectrum. The resulting limits on $C_{U\mu}$ and $C_{D\mu}$ are very similar to those obtained in the MFV scenario (see Fig. 3) and are required to be much smaller than the allowed range for $C_{b\mu}$.

In the lower panel of Fig. 4 we show the present and projected limits in the $C_{b\mu}$–λ_{bs} plane (here we set $C_{D\mu} = C_{U\mu} = 0$, after checking that no large correlation with them is present). As for the MFV case, the fit of the flavor anomalies in Eq. (10) combined with the upper limit on $|C_{b\mu}|$, provides a lower bound on $|\lambda_{bs}|$. In this case, while at present this limit is much lower than the natural value predicted from $U(2)$ symmetry, $\lambda_{bs} \sim V_{ts}$, with high luminosity an interesting region will be probed. For example, in the $U(2)$ flavor models of Refs. [29,33,34,57] a small value of λ_{bs} is necessary in order to pass the bounds from $B - \bar{B}$ mixing.

3. Single-operator benchmarks

It is illustrative to show the limits on λ_{bs}^q when only one flavor-diagonal coefficient $C_{q\mu}$ is non-vanishing, while fitting at the same time ΔC_9^μ in Eq. (10). The expected 2σ limits with 36.1 fb^{-1} (3000 fb^{-1}) are

$$\begin{aligned}
\lambda_{bs}^u &> 0.072\ (0.77), \quad \lambda_{bs}^u < -0.097\ (-0.76),\\
\lambda_{bs}^d &> 0.049\ (0.36), \quad \lambda_{bs}^d < -0.032\ (-0.34),\\
\lambda_{bs}^s &> 0.007\ (0.04), \quad \lambda_{bs}^s < -0.004\ (-0.03),\\
\lambda_{bs}^c &> 0.003\ (0.02), \quad \lambda_{bs}^c < -0.004\ (-0.02),\\
\lambda_{bs}^b &> 0.002\ (0.01), \quad \lambda_{bs}^b < -0.002\ (-0.006).
\end{aligned} \tag{16}$$

3.2 Model examples

We briefly speculate on the UV scenarios capable of explaining the observed pattern of deviations in the rare B meson decays. For our EFT approach to be valid, we focus on models with new resonances beyond the kinematical reach for threshold production at the LHC. In such models, the effective operators in Eq. (1) are presumably generated at the tree level.[4] We focus here on the single mediator models in which the required effect is obtained by integrating out a single resonance. These include either an extra Z' bosons [29,33,38–52] or a leptoquark [28,53–62] (for a recent review on leptoquarks see [63]).

We note that a full set of single mediator models with tree-level matching to the vector triplet ($c^{(3)}_{Q_{ij}L_{kl}}$) or singlet ($c^{(1)}_{Q_{ij}L_{kl}}$) operators consists of color-singlet vectors $Z'_\mu \sim (\mathbf{1},\mathbf{1},0)$ and $W'_\mu \sim (\mathbf{1},\mathbf{3},0)$, color-triplet scalar $S_3 \sim (\bar{\mathbf{3}},\mathbf{3},1/3)$, and vectors $U_1^\mu \sim (\mathbf{3},\mathbf{1},2/3)$, $U_3^\mu \sim (\mathbf{3},\mathbf{3},2/3)$, in the notation of Ref. [63]. The quantum numbers in brackets indicate color, weak, and hypercharge representations, respectively.

Z' and W' models A color-singlet vector resonance gives rise to an s-channel resonant contribution to the dilepton invariant mass distributions if $M_{Z'}$ is kinematically accessible. Otherwise, the deviation in the tails is described well by the dimension-six operators in Eq. (1) with $\Lambda = M_V$ and

$$c^{(3)}_{Q_{ij}L_{kl}} = -g_Q^{(3),ij} g_L^{(3),kl}, \quad c^{(1)}_{Q_{ij}L_{kl}} = -g_Q^{(1),ij} g_L^{(1),kl}, \tag{17}$$

obtained after integrating out the heavy vectors with interactions $\mathcal{L} \supset Z'_\mu J_\mu + W'^a_\mu J^a_\mu$, where

$$\begin{aligned}
J_\mu &= g_Q^{(1),ij}(\bar{Q}_i \gamma_\mu Q_j) + g_L^{(1),kl}(\bar{L}_k \gamma^\mu L_l),\\
J^a_\mu &= g_Q^{(3),ij}(\bar{Q}_i \gamma_\mu \sigma^a Q_j) + g_L^{(3),kl}(\bar{L}_k \gamma^\mu \sigma^a L_l).
\end{aligned} \tag{18}$$

A quark flavor-violating $g_Q^{(x),23}$ coupling and $g_L^{(x),22}$ are required to explain the flavor anomalies, while the limits from $pp \to \mu^+\mu^-$ reported in Table 1 can easily be translated to the flavor-diagonal couplings and mass combinations.

For example, assuming a singlet Z' with $g_Q^{(1),ii} = g_L^{(1),ii} = g_*$ and MFV structure ($g_Q^{(1),23} = V_{ts} g_*$), as dictated by neutral meson oscillation constraints, we derive limits on g_* as a function of the mass $M_{Z'}$, both fitting the data directly in the full model,[5] and in the EFT approach. The results are shown in Fig. 5. The limits in the full model are shown with solid-blue and those in the EFT are shown with dashed-blue. We see that for a mass $M_{Z'} \gtrsim 4 - 5$ TeV the limits in the two approaches agree well but for the lower masses the EFT still provide conservative bounds.[6] On top of this we show with green lines the best fit and 2σ interval that reproduces the $b \to s\mu\mu$ flavor anomalies, showing how LHC dimuon searches already exclude such a scenario independently of the Z' mass. The red solid line indicates the naive bound obtained when interpreting the limits on the narrow-width resonance production $\sigma(pp \to Z') \times \mathcal{B}(Z' \to \mu^+\mu^-)$ from Fig. 6 of Ref. [11].

Related to the above analysis we comment on the model recently proposed in Ref. [52]. An anomaly-free horizontal gauge symmetry is introduced, with a corresponding gauge field (Z'_h) having MFV-like couplings in the quark sector. Figure 1 of Ref. [52] shows the preferred region from ΔC_9^μ

[4] Note that including a loop suppression factor of $\sim \frac{1}{16\pi^2}$, the fit of the flavor anomalies in Eq. (10) points to a scale $\Lambda \approx 2.6^{+0.2}_{-0.3}$ TeV (see for example models proposed in Refs. [35–37]).

[5] The Z' decay width is determined by decays into the SM fermions $u, d, s, c, b, t, \mu, \nu_\mu$ via Eq. (18), i.e. $\Gamma_{Z'}/M_{Z'} = 5g_*^2/(6\pi)$.

[6] See Ref. [9] for a more detailed discussion on the EFT validity in high-p_T dilepton tails.

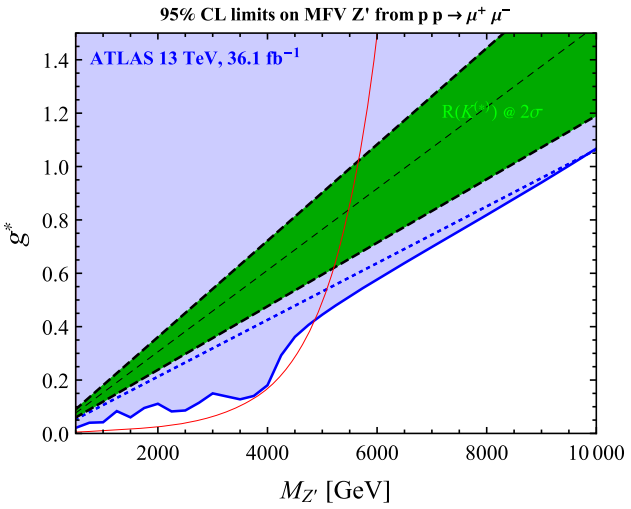

Fig. 5 Limits on the Z' MFV model from $pp \to \mu^+\mu^-$. See text for details

in the mass versus coupling plane, as well as the constraint from the Z' resonance search (from the same experimental analysis used here [11]). While the limits from the resonance search are effective up to ~ 4 TeV, we note that the limits from the tails go even beyond and are expected to probe all of the interesting parameter space of this model with the future-projected LHC data. Note that this statement is independent of the Z' mass (as long as the EFT is valid).

Leptoquark models A color-triplet resonance in the t-channel gives rise to $pp \to \ell^+\ell^-$ at the LHC [64–66]. The relevant interaction Lagrangian for explaining B decay anomalies is

$$\mathcal{L} \supset y^{LL}_{3ij}\,\bar{Q}^{c,i}_L i\sigma^2\sigma^a L^j_L S^a_3 + x^{LL}_{3ij}\,\bar{Q}^i_L\gamma^\mu\sigma^a L^j_L U^a_{3,\mu} + x^{LL}_{1ij}\,\bar{Q}^i_L\gamma^\mu L^j_L U_{1,\mu} + \text{h.c.}, \tag{19}$$

and the matching to the EFT is provided in Table 4 of Ref. [63]. The constraints from Table 1 apply again in a straightforward way. The validity of the expansion has been studied in details in Refs. [64,65]. We would like to point out that similar limits would apply even for a relatively light LQ (in the $\sim$ TeV range). As an illustration, the fit to low-energy anomalies in the model of Ref. [37] (where the effect is loop-generated), requires large charm–muon–LQ coupling, leading to a potentially observable $c\,\bar{c} \to \mu^+\mu^-$ production at high-p_T. We also note that the single LQ production at the LHC can constrain similar couplings [67].

4 Conclusions

In this work we discuss the contribution from flavor non-universal new physics to the high-p_T dilepton tails in $pp \to \ell^+\ell^-$, where $\ell = e, \mu$. In particular, we set the best up-to-date limits on all 36 chirality-conserving four-fermion operators in the SMEFT which contribute to these processes by recasting ATLAS analysis at 13 TeV with 36.1 fb^{-1} of data, as well as estimate the final sensitivity for the high-luminosity phase at the LHC.

Recent results in rare semileptonic B meson decays show some intriguing hints for possible violation of lepton-flavor universality beyond the SM. It is particularly interesting to notice that several anomalies coherently point toward a new physics contribution in the left-handed $b_L \to s_L\mu^+_L\mu^-_L$ contact interaction. In most flavor models, the flavor-changing interactions are related (and usually suppressed with respect) to the flavor-diagonal ones. These in turn, are probed via the high-p_T dimuon tail, allowing us to already set relevant limits on the parameter space of some models.

In particular, our limits exclude or put in strong tension, scenarios which aim to describe the flavor anomalies using MFV structure that directly relates the $bs\mu\mu$ contact interaction to the ones involving first generation quarks, tightly constrained from $pp \to \mu^+\mu^-$. On the other hand, scenarios with $U(2)_Q$ flavor symmetry predominantly coupled to the third generation quarks lead to milder constraints. In order to further illustrate our point, we discuss a few explicit examples with heavy mediator states (colorless vectors and leptoquarks) and show a comparison of the limits obtained in the EFT with those obtained directly in the model.

If the flavor anomalies get confirmed with more data, correlated signals in high-p_T processes at the LHC will be crucial in order to decipher the responsible dynamics. We show how high-energy dilepton tails provide very valuable information in this direction.

Acknowledgements We would like to thank Martín González-Alonso and Gino Isidori for useful discussions. This work is supported in part by the Swiss National Science Foundation (SNF) under contract 200021-159720.

Open Access This article is distributed under the terms of the Creative Commons Attribution 4.0 International License (http://creativecommons.org/licenses/by/4.0/), which permits unrestricted use, distribution, and reproduction in any medium, provided you give appropriate credit to the original author(s) and the source, provide a link to the Creative Commons license, and indicate if changes were made.
Funded by SCOAP^3.

Appendix A: Dilepton cross section

The unpolarized partonic differential cross section following from Eq. (2) is given by

$$\frac{\mathrm{d}\hat{\sigma}}{\mathrm{d}t} = \frac{1}{48\pi s^2}\,u^2\left(|F_{q_L\ell_L}(s)|^2 + |F_{q_R\ell_R}(s)|^2\right) + \frac{1}{48\pi s^2}\,t^2\left(|F_{q_L\ell_R}(s)|^2 + |F_{q_R\ell_L}(s)|^2\right), \tag{A.1}$$

where s, t, and u are the Mandelstam variables. The total partonic cross section is

$$\hat{\sigma} = \frac{s}{144\pi}\big(|F_{q_L\ell_L}(s)|^2 + |F_{q_R\ell_R}(s)|^2 + |F_{q_L\ell_R}(s)|^2 + |F_{q_R\ell_L}(s)|^2\big), \tag{A.2}$$

while the hadronic cross section is obtained after convoluting the partonic one with the corresponding parton luminosity functions

$$\mathcal{L}_{q\bar{q}}(\tau,\mu_F) = \int_\tau^1 \frac{\mathrm{d}x}{x}\, f_q(x,\mu_F) f_{\bar{q}}(\tau/x,\mu_F). \tag{A.3}$$

In particular, the cross section in the dilepton invariant mass bin $\left[\tau_{\min}^{\text{bin}}, \tau_{\max}^{\text{bin}}\right]$ is given by

$$\sigma^{\text{bin}}(p\ p\to\ell^+\ell^-) = \sum_q \int_{\tau_{\min}^{\text{bin}}}^{\tau_{\max}^{\text{bin}}} \mathrm{d}\tau\ 2\mathcal{L}_{q\bar{q}}(\tau,\mu_F)\,\hat{\sigma}(\tau s_0). \tag{A.4}$$

Appendix B: Operator limits

In Table 1 we show the present 2σ limits on the 36 independent four-fermion operators contributing to $pp \to \ell^+\ell^-$ from the 13 TeV ATLAS analysis [11] with 36.1 fb^{-1} of data, as well as projections for 3000 fb^{-1}, where only one operator is turned on at a time. The notation used is as in Eq. (1) but the cutoff dependence has been reabsorbed as $C_x \equiv \frac{v^2}{\Lambda^2} c_x$. In the case of operators involving b_L quark instead, we keep only the combination of triplet and singlet aligned with it, since the top quark does not enter in this observable. In the Gaussian approximation we derived the correlation matrix in the 36 coefficients and checked that the only non-negligible correlation is the one among the triplet and singlet $(\bar{L}L)(\bar{L}L)$ operators with the same fermion content. This correlation is shown explicitly in the 2d fit of Fig. 3.

Table 1 One-parameter 2σ limits from $pp \to \mu^+\mu^-, e^+e^-$

C_i	ATLAS 36.1 fb^{-1}	3000 fb^{-1}
$C^{(1)}_{Q^1L^2}$	$[-5.73, 14.2] \times 10^{-4}$	$[-1.30, 1.51] \times 10^{-4}$
$C^{(3)}_{Q^1L^2}$	$[-7.11, 2.84] \times 10^{-4}$	$[-5.25, 5.25] \times 10^{-5}$
$C_{u_RL^2}$	$[-0.84, 1.61] \times 10^{-3}$	$[-2.00, 2.66] \times 10^{-4}$
$C_{u_R\mu_R}$	$[-0.52, 1.36] \times 10^{-3}$	$[-1.04, 1.08] \times 10^{-4}$
$C_{Q^1\mu_R}$	$[-0.82, 1.27] \times 10^{-3}$	$[-2.25, 4.10] \times 10^{-4}$
$C_{d_RL^2}$	$[-2.13, 1.61] \times 10^{-3}$	$[-8.98, 5.11] \times 10^{-4}$
$C_{d_R\mu_R}$	$[-2.31, 1.34] \times 10^{-3}$	$[-4.89, 3.33] \times 10^{-4}$
$C^{(1)}_{Q^2L^2}$	$[-8.84, 7.35] \times 10^{-3}$	$[-3.83, 2.39] \times 10^{-3}$
$C^{(3)}_{Q^2L^2}$	$[-9.75, 5.56] \times 10^{-3}$	$[-1.43, 1.15] \times 10^{-3}$
$C_{Q^2\mu_R}$	$[-7.53, 8.67] \times 10^{-3}$	$[-2.58, 3.73] \times 10^{-3}$
$C_{s_RL^2}$	$[-1.04, 0.93] \times 10^{-2}$	$[-4.42, 3.33] \times 10^{-3}$
$C_{s_R\mu_R}$	$[-1.09, 0.87] \times 10^{-2}$	$[-4.67, 2.73] \times 10^{-3}$
$C_{c_RL^2}$	$[-1.33, 1.52] \times 10^{-2}$	$[-4.58, 6.54] \times 10^{-3}$
$C_{c_R\mu_R}$	$[-1.21, 1.62] \times 10^{-2}$	$[-3.48, 6.32] \times 10^{-3}$
$C_{b_LL^2}$	$[-2.61, 2.07] \times 10^{-2}$	$[-11.1, 6.33] \times 10^{-3}$
$C_{b_L\mu_R}$	$[-2.28, 2.42] \times 10^{-2}$	$[-8.53, 10.0] \times 10^{-3}$
$C_{b_RL^2}$	$[-2.41, 2.29] \times 10^{-2}$	$[-9.90, 8.68] \times 10^{-3}$
$C_{b_R\mu_R}$	$[-2.47, 2.23] \times 10^{-2}$	$[-10.5, 7.97] \times 10^{-3}$
$C^{(1)}_{Q^1L^1}$	$[-0.0, 1.75] \times 10^{-3}$	$[-1.01, 1.13] \times 10^{-4}$
$C^{(3)}_{Q^1L^1}$	$[-8.92, -0.54] \times 10^{-4}$	$[-3.99, 3.93] \times 10^{-5}$
$C_{u_RL^1}$	$[-0.19, 1.92] \times 10^{-3}$	$[-1.56, 1.92] \times 10^{-4}$
$C_{u_Re_R}$	$[0.15, 2.06] \times 10^{-3}$	$[-7.89, 8.23] \times 10^{-5}$
$C_{Q^1e_R}$	$[-0.40, 1.37] \times 10^{-3}$	$[-1.8, 2.85] \times 10^{-4}$
$C_{d_RL^1}$	$[-2.1, 1.04] \times 10^{-3}$	$[-7.59, 4.23] \times 10^{-4}$
$C_{d_Re_R}$	$[-2.55, 0.46] \times 10^{-3}$	$[-3.37, 2.59] \times 10^{-4}$
$C^{(1)}_{Q^2L^1}$	$[-6.62, 4.36] \times 10^{-3}$	$[-3.31, 1.92] \times 10^{-3}$
$C^{(3)}_{Q^2L^1}$	$[-8.24, 2.05] \times 10^{-3}$	$[-8.87, 7.90] \times 10^{-4}$
$C_{Q^2e_R}$	$[-4.67, 6.34] \times 10^{-3}$	$[-2.11, 3.30] \times 10^{-3}$
$C_{s_RL^1}$	$[-7.4, 5.9] \times 10^{-3}$	$[-3.96, 2.8] \times 10^{-3}$
$C_{s_Re_R}$	$[-8.17, 5.06] \times 10^{-3}$	$[-3.82, 2.13] \times 10^{-3}$
$C_{c_RL^1}$	$[-0.83, 1.13] \times 10^{-2}$	$[-3.74, 5.77] \times 10^{-3}$
$C_{c_Re_R}$	$[-0.67, 1.27] \times 10^{-2}$	$[-2.59, 4.17] \times 10^{-3}$
$C_{b_LL^1}$	$[-1.93, 1.19] \times 10^{-2}$	$[-8.62, 4.82] \times 10^{-3}$
$C_{b_Le_R}$	$[-1.47, 1.67] \times 10^{-2}$	$[-7.29, 8.99] \times 10^{-3}$
$C_{b_RL^1}$	$[-1.65, 1.49] \times 10^{-2}$	$[-8.86, 7.48] \times 10^{-3}$
$C_{b_Re_R}$	$[-1.73, 1.40] \times 10^{-2}$	$[-9.38, 6.63] \times 10^{-3}$

References

1. G. Isidori, Y. Nir, G. Perez, Ann. Rev. Nucl. Part. Sci. **60**, 355 (2010). arXiv:1002.0900 [hep-ph]
2. R. Aaij et al., [LHCb Collaboration], Phys. Rev. Lett. **113**, 151601 (2014). arXiv:1406.6482 [hep-ex]
3. R. Aaij et al., [LHCb Collaboration], Phys. Rev. Lett. **111**, 191801 (2013). arXiv:1308.1707 [hep-ex]
4. R. Aaij et al., [LHCb Collaboration], JHEP **1602**, 104 (2016). arXiv:1512.04442 [hep-ex]
5. S. Bifani, in Seminar at CERN, April 18th (2017)
6. V. Cirigliano, M. Gonzalez-Alonso, M.L. Graesser, JHEP **1302**, 046 (2013). arXiv:1210.4553 [hep-ph]
7. M. Gonzlez-Alonso, J. Martin Camalich, arXiv:1606.06037 [hep-ph]
8. J. de Blas, M. Chala, J. Santiago, Phys. Rev. D **88**, 095011 (2013). arXiv:1307.5068 [hep-ph]
9. M. Farina, G. Panico, D. Pappadopulo, J.T. Ruderman, R. Torre, A. Wulzer. arXiv:1609.08157 [hep-ph]
10. D.A. Faroughy, A. Greljo, J.F. Kamenik, Phys. Lett. B **764**, 126 (2017). arXiv:1609.07138 [hep-ph]
11. The ATLAS collaboration [ATLAS Collaboration], ATLAS-CONF-2017-027
12. B. Grzadkowski, M. Iskrzynski, M. Misiak, J. Rosiek, JHEP **1010**, 085 (2010). arXiv:1008.4884 [hep-ph]
13. A. Efrati, A. Falkowski, Y. Soreq, JHEP **1507**, 018 (2015). arXiv:1503.07872 [hep-ph]
14. G. Cowan, K. Cranmer, E. Gross, O. Vitells, Eur. Phys. J. C **71**, 1554 (2011) (Erratum: [Eur. Phys. J. C **73** (2013) 2501] arXiv:1007.1727 [physics.data-an])
15. L.A. Harland-Lang, A.D. Martin, P. Motylinski, R.S. Thorne, Eur. Phys. J. C **75**(5), 204 (2015). arXiv:1412.3989 [hep-ph]
16. A. Alloul, N.D. Christensen, C. Degrande, C. Duhr, B. Fuks, Comput. Phys. Commun. **185**, 2250 (2014). arXiv:1310.1921 [hep-ph]
17. J. Alwall et al., JHEP **1407**, 079 (2014). arXiv:1405.0301 [hep-ph]
18. B. Capdevila, A. Crivellin, S. Descotes-Genon, J. Matias, J. Virto. arXiv:1704.05340 [hep-ph]
19. W. Altmannshofer, P. Stangl, D.M. Straub. arXiv:1704.05435 [hep-ph]
20. L.S. Geng, B. Grinstein, S. Jager, J. Martin Camalich, X.L. Ren, R.X. Shi. arXiv:1704.05446 [hep-ph]
21. M. Ciuchini, A.M. Coutinho, M. Fedele, E. Franco, A. Paul, L. Silvestrini, M. Valli. arXiv:1704.05447 [hep-ph]
22. S. Descotes-Genon, J. Matias, M. Ramon, J. Virto, JHEP **1301**, 048 (2013). arXiv:1207.2753 [hep-ph]
23. G. Hiller, F. Kruger, Phys. Rev. D **69**, 074020 (2004). arXiv:hep-ph/0310219
24. C. Bobeth, G. Hiller, G. Piranishvili, JHEP **0712**, 040 (2007). arXiv:0709.4174 [hep-ph]
25. M. Bordone, G. Isidori, A. Pattori, Eur. Phys. J. C **76**(8), 440 (2016). arXiv:1605.07633 [hep-ph]
26. A. Celis, J. Fuentes-Martin, A. Vicente, J. Virto. arXiv:1704.05672 [hep-ph]
27. B. Bhattacharya, A. Datta, D. London, S. Shivashankara, Phys. Lett. B **742**, 370 (2015). arXiv:1412.7164 [hep-ph]
28. R. Alonso, B. Grinstein, J. Martin Camalich, JHEP **1510**, 184 (2015). arXiv:1505.05164 [hep-ph]
29. A. Greljo, G. Isidori, D. Marzocca, JHEP **1507**, 142 (2015). arXiv:1506.01705 [hep-ph]
30. C. Patrignani et al., [Particle Data Group], Chin. Phys. C **40**(10), 100001 (2016)
31. G. D'Ambrosio, G.F. Giudice, G. Isidori, A. Strumia, Nucl. Phys. B **645**, 155 (2002). arXiv:hep-ph/0207036
32. R. Barbieri, G. Isidori, J. Jones-Perez, P. Lodone, D.M. Straub, Eur. Phys. J. C **71**, 1725 (2011). arXiv:1105.2296 [hep-ph]
33. D. Buttazzo, A. Greljo, G. Isidori, D. Marzocca, JHEP **1608**, 035 (2016). arXiv:1604.03940 [hep-ph]
34. M. Bordone, G. Isidori, S. Trifinopoulos. arXiv:1702.07238 [hep-ph]
35. J.F. Kamenik, Y. Soreq, J. Zupan. arXiv:1704.06005 [hep-ph]
36. P. Arnan, L. Hofer, F. Mescia, A. Crivellin, JHEP **1704**, 043 (2017). doi:10.1007/JHEP04(2017)043. arXiv:1608.07832 [hep-ph]
37. D. Bečirević, O. Sumensari. arXiv:1704.05835 [hep-ph]
38. R. Gauld, F. Goertz, U. Haisch, JHEP **1401**, 069 (2014). arXiv:1310.1082 [hep-ph]
39. A.J. Buras, F. De Fazio, J. Girrbach, JHEP **1402**, 112 (2014). arXiv:1311.6729 [hep-ph]
40. W. Altmannshofer, S. Gori, M. Pospelov, I. Yavin, Phys. Rev. D **89**, 095033 (2014). arXiv:1403.1269 [hep-ph]
41. A. Crivellin, G. D'Ambrosio, J. Heeck, Phys. Rev. Lett. **114**, 151801 (2015). arXiv:1501.00993 [hep-ph]
42. A. Crivellin, G. D'Ambrosio, J. Heeck, Phys. Rev. D **91**(7), 075006 (2015). arXiv:1503.03477 [hep-ph]
43. A. Celis, J. Fuentes-Martin, M. Jung, H. Serodio, Phys. Rev. D **92**(1), 015007 (2015). arXiv:1505.03079 [hep-ph]
44. A. Falkowski, M. Nardecchia, R. Ziegler, JHEP **1511**, 173 (2015). arXiv:1509.01249 [hep-ph]
45. S.M. Boucenna, A. Celis, J. Fuentes-Martin, A. Vicente, J. Virto, Phys. Lett. B **760**, 214 (2016). arXiv:1604.03088 [hep-ph]
46. A. Crivellin, J. Fuentes-Martin, A. Greljo, G. Isidori, Phys. Lett. B **766**, 77 (2017). arXiv:1611.02703 [hep-ph]
47. B. Allanach, F.S. Queiroz, A. Strumia, S. Sun, Phys. Rev. D **93**(5), 055045 (2016). arXiv:1511.07447 [hep-ph]
48. C.W. Chiang, X.G. He, G. Valencia, Phys. Rev. D **93**(7), 074003 (2016). arXiv:1601.07328 [hep-ph]
49. A. Carmona, F. Goertz, Phys. Rev. Lett. **116**(25), 251801 (2016). arXiv:1510.07658 [hep-ph]
50. C. Niehoff, P. Stangl, D.M. Straub, Phys. Lett. B **747**, 182 (2015). arXiv:1503.03865 [hep-ph]
51. E. Megias, G. Panico, O. Pujolas, M. Quiros, JHEP **1609**, 118 (2016). arXiv:1608.02362 [hep-ph]
52. R. Alonso, P. Cox, C. Han,T.T. Yanagida. arXiv:1704.08158 [hep-ph]
53. G. Hiller, M. Schmaltz, JHEP **1502**, 055 (2015). arXiv:1411.4773 [hep-ph]
54. I. de Medeiros Varzielas, G. Hiller, JHEP **1506**, 072 (2015). arXiv:1503.01084 [hep-ph]
55. S. Fajfer, N. Konik, Phys. Lett. B **755**, 270 (2016). arXiv:1511.06024 [hep-ph]
56. B. Gripaios, M. Nardecchia, S.A. Renner, JHEP **1505**, 006 (2015). arXiv:1412.1791 [hep-ph]
57. R. Barbieri, G. Isidori, A. Pattori, F. Senia, Eur. Phys. J. C **76**(2), 67 (2016). arXiv:1512.01560 [hep-ph]
58. R. Barbieri, C.W. Murphy, F. Senia, Eur. Phys. J. C **77**(1), 8 (2017). arXiv:1611.04930 [hep-ph]
59. H. Ps, E. Schumacher, Phys. Rev. D **92**(11), 114025 (2015). arXiv:1510.08757 [hep-ph]
60. M. Bauer, M. Neubert, Phys. Rev. Lett. **116**(14), 141802 (2016). arXiv:1511.01900 [hep-ph]
61. D. Bečirević, N. Košnik, O. Sumensari, R. Zukanovich Funchal, JHEP **1611**, 035 (2016). arXiv:1608.07583 [hep-ph]
62. G. Hiller, I. Nisandzic. arXiv:1704.05444 [hep-ph]
63. I. Doršner, S. Fajfer, A. Greljo, J.F. Kamenik, N. Košnik, Phys. Rep. **641**, 1 (2016). arXiv:1603.04993 [hep-ph]
64. S. Davidson, S. Descotes-Genon, P. Verdier, Phys. Rev. D **91**(5), 055031 (2015). arXiv:1410.4798 [hep-ph]

65. A. Bessaa, S. Davidson, Eur. Phys. J. C **75**(2), 97 (2015). arXiv:1409.2372 [hep-ph]
66. N. Raj, Phys. Rev. D **95**(1), 015011 (2017). arXiv:1610.03795 [hep-ph]
67. I. Dorsner, S. Fajfer, A. Greljo, JHEP **1410**, 154 (2014). arXiv:1406.4831 [hep-ph]